Higher Order Loop Corrections for Short Range Magnetoquasistatic Position Tracking

Darmindra D. Arumugam, *Student Member, IEEE,* Joshua D. Griffin, *Member, IEEE,*
Daniel D. Stancil, *Fellow, IEEE,* and David S. Ricketts, *Member, IEEE*

***Abstract*—Magnetoquasistatic position tracking has been shown to be an excellent technique to measure distances between an emitting and receiving loop for distances up to 50 m along a direction perpendicular to the surface normal of the loops [1]. For short distances from the emitting loop (i.e., less than about ten loop radii) there is an error in the estimated distance. In this paper, we examine the cause of this error and show that a significant portion is due to the simplification of the emitting loop as a simple magnetic dipole. By including a more accurate expression of the source field, errors can be significantly reduced. We show that the first correction term results in a reduction in rms and peak distance estimation error of 12.51 cm (54.44 %) and 11.27 cm (44.72 %), respectively, for distances less than 1.5δ, where δ is the skin depth.**

***Index Terms*—Electromagnetic fields, magnetoquasistatics, radio tracking, radio position measurement.**

I. Introduction

Wireless position tracking is an important technology for a wide array of applications such as navigation and asset-tracking [2], [3]. Despite numerous advances, current systems suffer reduced performance in non-line-of-sight (NLoS) environments [2] and when in proximity to lossy objects such as the human body. Recently, a position tracking technique using magnetoquasistatic fields has been proposed and experimentally demonstrated [1]. This approach allows for NLoS position tracking in a wide range of environments since many obstructions can be modeled as non-magnetic dielectrics, e.g. the human body, that do not significantly perturb the fields. In this approach, a magnetoquasistatic field is generated by exciting an emitting loop with a sinusoidal signal source and detected by a receiving loop with known position and orientation (see Fig. 1). The measured voltage at the terminal of the receiving loop is a function of the distance between the emitting and receiving loops. By inverting the theoretical expression for field measured by the receiving antenna, the distance can be determined [1].

Unfortunately, many position tracking applications are not in free space, but occur on or near a conducting medium, such as the earth's surface. The presence of a conducting region significantly modifies the fields measured by the receiving loop since the emitting loop not only directly produces the fields seen by the receiver, but also induces currents in the conducting region that produce secondary fields, which are also seen by the receiver. Several techniques exist for correcting for the conductive region's affect, such as classical image theory or, as was demonstrated recently, complex image theory [1]. Figure 2 compares the accuracy of these methods with experimental measurements (see Sec. IV), where the loops are modeled as infinitesimal dipoles. It can be clearly seen that complex image theory provides increased accuracy over the free space and classical image theory models. While complex image theory does provide very good accuracy at large distances ($>$ 5 skin depths, δ), Fig. 2 shows that these errors increase at short distances. In this paper, we examine the validity of the

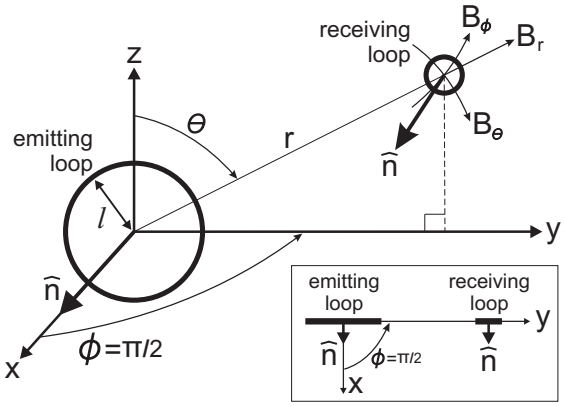

Fig. 1. Coupling between an emitting loop at the origin of a spherical coordinate system and a receiving loop. Both loops reside on the y-z plane and have surface normals parallel to the x-y plane.

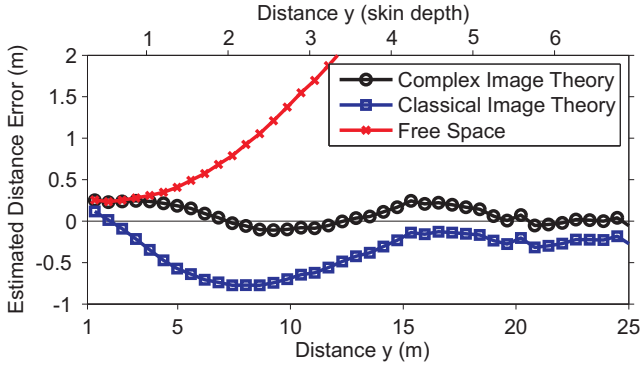

Fig. 2. Comparison of estimated distance error from inverting the theoretical expressions for complex image theory, classical image theory, and free space theory [using dipole fields for $m = 0$, see (2)]. The estimated distance error is found by the difference between the optimal solution of distance y and the measured distance.

D.D. Arumugam is with the Department of Electrical and Computer Engineering, Carnegie Mellon University, Pittsburgh, PA, 15213 USA e-mail: darumugam@cmu.edu

J.D. Griffin is with Disney Research, Pittsburgh, PA, 15213 USA e-mail: joshdgriffin@disneyresearch.com

D.D. Stancil is with the Department of Electrical and Computer Engineering, North Carolina State University, Raleigh, NC, 27695 USA e-mail: ddstancil@ncsu.edu

D.S. Ricketts is with the Department of Electrical and Computer Engineering, Carnegie Mellon University, Pittsburgh, PA, 15213 USA e-mail: ricketts@ece.cmu.edu

infinitesimal dipole approximation to understand the origin of these errors and how they can be reduced.

II. Complex Image Theory

We begin by briefly reviewing the main concepts of complex image theory to lay the foundation for our measurements, calculations, and corrections for short range distance estimation. The fields generated by an arbitrary source at $z = h$ in the presence of earth ($z \leq 0$), shown two-dimensionally in Fig. 3, are a function of the fields from the source, its image at a complex depth beneath the ground (referred to as the complex image), and a summation of correction terms [4]. The correction terms are increasingly negligible at distances greater than a skin depth from the classical image, i.e., when $R^0 > \delta$, where R^0 is the distance from the classical image of the source. The magnetic induction is [4]

$$\vec{B}_p(x,y,z) \approx \vec{B}_p^s(x,y,z) + c_p \vec{B}_p^i(x,y,z), \tag{1}$$

where the first and second terms are due to the source and complex image, respectively. The subscript $p = ||, \perp$ indicates the components parallel and perpendicular to the ground, respectively; the superscripts s and i indicate the source and the complex image, respectively; and $c_{||} = 1$ and $c_\perp = -1$. The magnetic induction of the source and complex image in Fig. 3 are $\vec{B}^s(x,y,z) = \vec{B}^l(x,y,z-h)$ and $\vec{B}^i(x,y,z) = \vec{B}^l(x,y,-z-h-\alpha)$, where $\vec{B}^l(x,y,z)$ is the magnetic induction of the emitting loop at the origin expressed in cartesian coordinates, $\alpha = \delta(1-j)$, $\delta = 1/\sqrt{\pi f \mu_0 \sigma}$ is the skin depth, σ is the ground conductivity, μ_0 is the permeability of free space, and f is the frequency. For the specific two-dimensional case in Fig. 3, only the B_ϕ components (or in cartesian coordinates, the B_x components) are of concern.

III. Coupling and Fields of a Loop

We now examine more closely the fields generated by an emitting loop antenna and the signal induced on a receiving loop antenna, Fig. 1 and 3. In our model, we simplify our system by assuming that one loop is large and one is small, i.e. the distance y in Fig. 3 is > 10 radii of the small loop but < 5 radii of the large loop. This allows us calculate the exact fields for the large loop only and assume the small loop has a uniform field over its cross section. Due to the reciprocity of the system and the fact that distance is an absolute measurement, one could consider a large emitting loop and a small receiving loop or visa versa. We choose a large emitting loop and small receiving loop for our calculations to enable the use of existing exact expressions for the magnetic field of a finite current loop, and avoid the integration of a non-uniform field over the receiving loop.

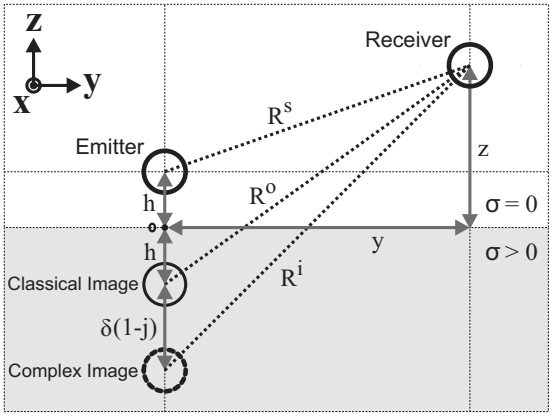

Fig. 3. The y-z plane of Fig. 1 showing image locations for magnetoquasistatic fields generated by a source above a conducting earth [1].

The coupling between two loops, vertically situated in the y-z plane, Fig. 1, can be described using Faraday's law and the fields of the loop. The voltage generated at the terminals of a receiving, electrically-small, single-loop coil (assuming time-harmonic fields), is expressed as $V = -j\omega a_r(\hat{n} \cdot \vec{B})$, where $\omega = 2\pi f$, f is the oscillation frequency, a_r is the area of the receiving loop, and $\vec{B}$ is the magnetic induction of the emitting loop [5]:

$$\begin{aligned} B_r &= \frac{\mu_0 I l}{2r} \sum_{m=0}^{\infty} \frac{(-1)^m (2m+1)!!}{2^m m!} \frac{l^{2m+1}}{r^{2m+2}} P_{2m+1}(\cos\ \phi), \\ B_\phi &= \frac{-\mu_0 I l^2}{4r^3} \sum_{m=0}^{\infty} \frac{(-1)^m (2m+1)!!}{2^m (m+1)!} \left(\frac{l}{r}\right)^{2m} P_{2m+1}^1(\cos\ \phi), \\ B_\theta &= 0, \end{aligned} \tag{2}$$

where I is the current in the emitting loop, l is the radius of the emitting loop, r is the distance from the center of the emitting loop to the point of observation, ϕ is the angle of the loop makes from the x-axis, and P is the Legendre polynomial. Eq. (2) is valid for $r > l$. For the geometry shown in Fig. 1, B_r is parallel with the loop, and as a result, does not induce any voltage; only B_ϕ induces a voltage in the receiving loop and must be considered in (2). For $r >> l$, only the $m = 0$ term is important, and the fields are that of a magnetic dipole as used in [1]. Figure 4a is a plot of the calculated power detected at the receiving loop for distances of up to five radii (l) in the y direction ($I = 1$ A, $l = 1$ m, $a_r = 1$ m^2, $f =$ 387 kHz, 50 Ω impedance). Figure 4b is a plot of the change in power contributed by each additional term in (2). The change in power is increasingly negligible for higher order terms and greater distances. At smaller distances (< 3 radii) the second and higher order terms represent a noticeable correction.

IV. Measurements and Error Reduction

To determine the distance error at short ranges, we compared the theoretical induced signal at the receiving loop with the experimentally measured signal over a range of distances using the setup in Fig. 3 [1]. In our experiment, we used a small emitting loop and a large receiving loop, which is the reverse of our calculations. This was done to take advantage of a pre-existing test-setup. As mentioned previously, due to reciprocity, the distance measured in the experiment is equivalent to the distance calculated in the previous section.

The center height of the emitting and receiving loops, respectively, were $h = 0.84$ m and $z = 1.75$ m. The emitting loop was constructed using 45 turns of 34 AWG copper wire with a diameter of 16.5 cm and was driven at 387 kHz. The receiving loop was an active receiving loop (model LFL-1010

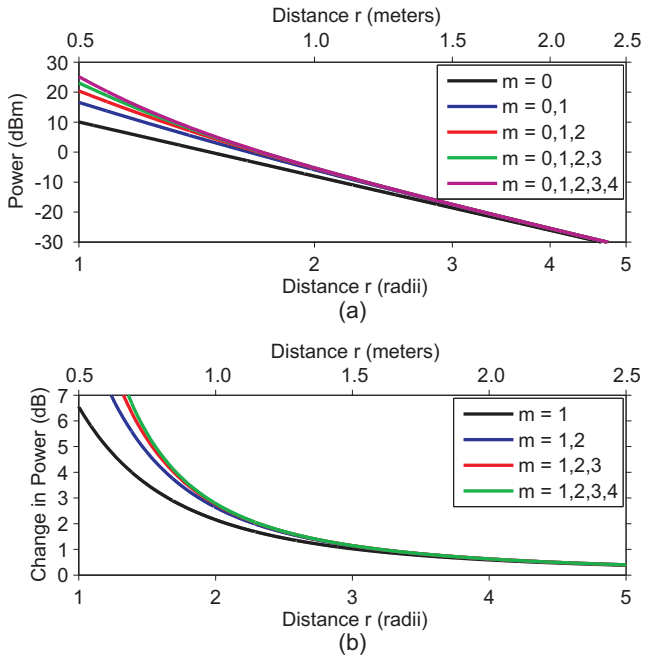

Fig. 4. Received power at the terminal of the receiving loop calculated for the coupling of the loops with a direction perpendicular to the surface normal of the loops, where $I = 1$ A, $l = 1$ m, $a_r = 1$ m^2, frequency of 387 kHz, and an impedance of 50 Ω is assumed.

from Wellbrook Communications) with a diameter of 1 m. A block diagram of the measurement system is shown in Fig. 5. A signal generator (E4433B Agilent), amplifier (ZFL-500+ MiniCircuits), and balun (ADT1-6AT-1 MiniCircuits) were used to drive the emitting loop. A spectrum analyzer (8593E Agilent) was used to measure the voltage at the terminals of the active receiving loop.

For the experimental geometry, the voltage at the terminals of the loop is expressed as $V = -j\omega a_r(\hat{n}\cdot(\vec{B}_{||}+\vec{B}_{\perp}))$, where $\vec{B}_{||}$ and $\vec{B}_{\perp}$ are defined in (1), and the magnetic induction of the larger loop is that in (2). For the setup depicted in Fig. 3, the only unknown variable is the distance y, where $r^2 = y^2 + (z-h)^2$ and $r = R^s$.

To compare the theoretical estimation to measured results, we need to calibrate our experimental system using a known distance. We chose a distance that is sufficiently far to consider both loops as magnetic dipoles. We placed the receiver 23.87 m from the emitting loop and measured the received power. We then calculated the theoretical power using complex image theory. The ratio of the measured and calculated power was used as a gain calibration in our system. All measurements used that same gain calibration constant as the antennas were moved from y =25 m to y =1 m.

Figure 6a is a plot of the estimated distance error, defined as the difference between the distance calculated using complex image theory and the measured distance, for the simple dipole approximation and the first two additional terms in (2) ($m = 0, 1, 2$). Figure 6b is a plot of the rms and peak position error as a function of number of the additional loop terms, for distances $y \leq 1.5\delta$, shown by the gray box in Fig 6a. The lowest-order additional loop term ($m = 1$) provides an rms and peak distance estimation error reduction of 12.51 cm (54.44 %) and 11.27 cm (44.72 %), respectively. The results show that, for short distances (i.e., less than about ten loop radii), the higher order terms of the complete field equations in (2) must be considered for accuracy, instead of the magnetic dipole approximation used in Fig. 2. For the measurements, this corresponds to approximate distances of $y \leq 1.5\delta$.

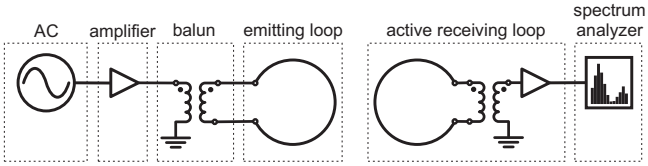

Fig. 5. Block diagram of the experimental measurement system [1].

V. Conclusions

The use of magnetoquasistatic fields analyzed with complex image theory enables long-range distance tracking [1]. At short distances ($y \leq 1.5\delta$), the lowest order additional term to the fields of a magnetic dipole provide an rms and peak distance estimation error reduction of 12.51 cm and 11.27 cm, respectively. This corresponds to an rms and peak distance estimation error percentage reduction of 54.44 % and 44.72 %, respectively.

References

[1] D. Arumugam, J. Griffin, and D. Stancil, "Experimental Demonstration of Complex Image Theory and Application to Position Measurement," *IEEE Antennas Wireless Propag. Lett.*, vol. 10, pp. 282 – 285, April 2011.

[2] K. Krizman, T. Biedka, and T. Rappaport, "Wireless Position Location: Fundamentals, Implementation Strategies, and Sources of Error," in *IEEE Vehicular Tech.*, vol. 47, no. 2, 1997, pp. 919–923.

[3] H. Liu, H. Darabi, P. Banerjee, and J. Liu, "Survey of Wireless Indoor Positioning Techniques and Systems," in *IEEE Trans. Sys., Man, and Cybernetics*, vol. 37, no. 6, November 2007, pp. 1067–1080.

[4] J. Weaver, "Image approximation for an arbitrary quasi-static field in the presence of a conducting half space," *Radio Science*, vol. 6, no. 6, pp. 647–653, June 1971.

[5] J. Jackson, "Classical Electrodynamics," John Wiley and Sons Inc., 1999.

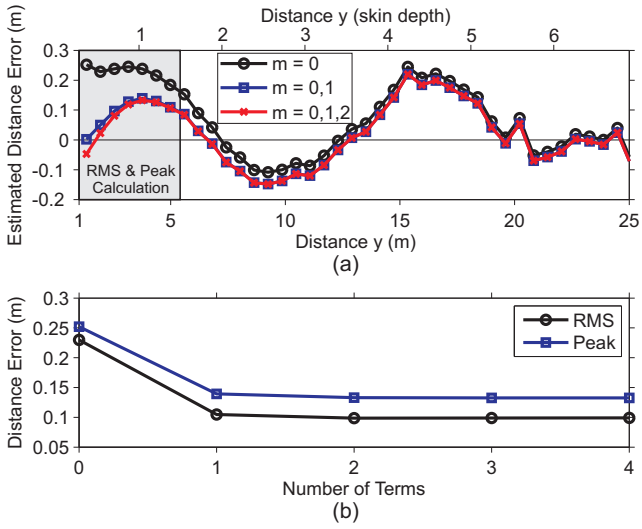

Fig. 6. Comparison of: (a) estimated distance error from inverting the theoretical expressions using the loop terms ($m = 0, 1, 2$). (b) rms distance error reduction using the additional loop terms, for distances $y \leq 1.5\delta$. The lowest-order additional loop term ($m = 1$) provides an rms and peak distance estimation error reduction of 12.51 cm (54.44 %) and 11.27 cm (44.72 %), respectively.